IEEE Access
Multidisciplinary | Rapid Review | Open Access Journal

Received 3 February 2023, accepted 17 February 2023, date of publication 22 February 2023, date of current version 1 March 2023.

Digital Object Identifier 10.1109/ACCESS.2023.3247796

RESEARCH ARTICLE

A Study of Reduced Torque Compensation Method Under Temperature Variation Based on Single Torque-Current Lookup Table

HYUN-JUN BAEK[1], SOON-HO KWON[2], DEUK-WON YOON[2], DO-HYUN KANG[3], (Graduate Student Member, IEEE), GEUN-HO LEE[1], AND HEE-SUN LIM[1]

[1]Department of Automotive Engineering, Kookmin University, Seoul 02707, South Korea
[2]Hyundai Mobis Company Ltd., Yongin-si 16891, Republic of Korea
[3]Department of Electrical and Computer Engineering, Sungkyunkwan University, Suwon 16419, Republic of Korea

Corresponding author: Hee-Sun Lim (popolhs@kookmin.ac.kr)

This work was supported in part by the Korea Institute for Advancement of Technology (KIAT); in part by the Human Resources Development (HRD) Program for Fostering Research and Development Specialists of Parts for Eco-Friendly Vehicle (xEV) under Grant P0017120; in part by the Korea Evaluation Institute of Industrial Technology (KEIT), South Korea; in part by the Development of 400kW Class Electric Drive System Technology Based on Multiple Motors for the Electrified Powertrain of Heavy Duty Fuel Cell Electric Trucks under Grant 20011866; and in part by the Development of 50∼150 kW Electric Drive System for Construction Machinery funded by Ministry of Trade, Industry and Energy (MOTIE), South Korea, under Grant 1055001018.

ABSTRACT In permanent magnet motors, the stator resistance and magnetic flux of the magnet change as the temperature increases. These changes result in a change in the maximum torque point per unit ampere (MTPA) of the motor. Without adequate compensation, this leads to a decrease in output torque. For this reason, look-up table (LUTs) are prepared over the temperature range and used for interpolation. This paper proposes a method to compensate for the output torque reduction due to a temperature increase using only a single LUT prepared at a base temperature. First, an estimation of the magnetic flux linkage and the output torque using a single LUT is performed. Second, the problem is modeled as a limited optimization problem to minimize the loss due to the torque reduction. The magnetic flux linkage and output torque are calculated in real time through the fundamental active power. The compensation value is calculated using the Lagrange multiplier method, an optimization technique, using the estimated magnetic flux linkage and output torque. The proposed method is verified by comparing it with other algorithms through simulation and experiment.

INDEX TERMS IPMSM, permanent magnet motor, active power, reactive power, torque compensation, Lagrange multiplier method, torque control.

I. INTRODUCTION

In addition to structural stability, IPMSMs are used in various industrial fields due to their high efficiency and power density due to additional reluctance torque. The torque equation of the IPMSM involves the magnetic flux, current, and inductance and is expressed as Equation (1). If the magnetic flux ϕ_f and inductances L_d and L_q are constant, the minimum currents I_d and I_q satisfying the torque can be determined through analytical methods [1]. These set currents are called the maximum torque point per unit ampere (MTPA).

$$T_e = \frac{3}{2}\frac{N_P}{2}\{\phi_f I_q + (L_d - L_q)I_d I_q\} \tag{1}$$

However, in Equation (1), ϕ_f, L_d and L_q are functions of temperature, and the motors used in harsh thermal environments, such as vehicle traction motors, occur parameter fluctuations due to temperature changes [2], [3], [4]. Since the MTPA calculation method using the analytical technique considers the parameters as constants, it does not reflect the fluctuations in operating points due to parameter changes with temperature. To overcome these limitations, a method of directly estimating and replacing parameters has been studied [5].

The associate editor coordinating the review of this manuscript and approving it for publication was R. K. Saket.

Reference [5] conducted real-time parameter estimation to compensate the output torque and proposed a method that combines the steepest descent technique to find the minimum value numerically and the affine projection technique, a type of adaptive filter.

In addition, methods employing mathematical models of IPMSMs such as [6] and [7] were proposed.

Reference [6] proposed a real-time parameter estimation through high-frequency injection based on the Levenberg-Marquardt method, and [7] proposed a method to find the optimal solution through numerical analysis methods such as Ferrari's method.

In the case of [5], [6], and [7], parameter estimation through additional observers or high-frequency injection was required. Here, the control performance is influenced by the observer's performance, and high-frequency injection causes voltage limitations, torque ripple, and additional losses.

In addition, there is a disadvantage that complex algorithms require substantial computational time. Moreover, precise parameter estimation through an observer is difficult due to various reasons such as magnetic saturation and cross coupling effects [4], [16].

Therefore, experiments mainly involve a method of creating an LUT for each temperature and then performing interpolation [8].

However, many experiments must be conducted to create an LUT for each temperature, resulting in time and material resource consumption. For this reason, [9] compensated for torque reduction caused by temperature changes of a motor based on a single LUT.

In [9], a torque command compensation technique using the change in the size of BEMF due to the change in magnetic flux was proposed by creating a LUT at intermediate temperature. Main idea of this is based on the change in the size of BEMF due to the change in magnetic flux. However, if the torque command is compensated only by the magnitude of the BEMF without considering the variation in parameter, an additional loss occurs because the LUT at intermediate temperature does not have information on the optimal operating point at the changed temperature.

The present proposes a method to compensate a current command using a single LUT created at a base temperature to move to an optimal driving point to overcome aforementioned limitations. This process is summarized as follows.

1) Development of an IPMSM model reflecting parameter changes according to temperature increase. The flux linkage and output torque are estimated using a single LUT.
2) Calculation of the compensation current command value using the Lagrange multiplier method along with the estimated flux linkage and output torque

This paper consists of five sections organized as follows. Section II analyzes the changes in motor parameters due to temperature increases and proposes a new IPMSM model that reflects these increases. Section III proposes a new estimation method for the flux linkage and output torque using the proposed IPMSM model and fundamental active power. The estimated flux linkage is verified using fundamental the reactive power, which eliminates the effects of the stator resistance. Section IV presents a method of calculating the compensation current command value by applying the Lagrange multiplier method to the estimated flux linkage and output torque. Finally, the proposed method is validated through simulations and experiments.

II. TEMPERATURE-DRIVEN PARAMETER CHANGES AND A NEW IPMSM MODEL

The motor is used to apply current to the stator to generate torque. However, applying current to the stator causes loss due to the stator resistance, which inevitably increases the motor temperature.

This section analyzes temperature-driven changes in the motor parameters and proposes a new IPMSM model that reflects these changes.

A. CHANGE IN THE STATOR RESISTANCE

The resistance is determined based on the resistivity, length, and cross-sectional area. However, the resistivity varies with temperature, causing the resistance to fluctuate as well.

TABLE 1. Resistance temperature coefficients of metals.

Material	Resistance Temperature Coefficient [Ω/°C]
Copper	0.004
Iron	0.006
Aluminum	0.0043

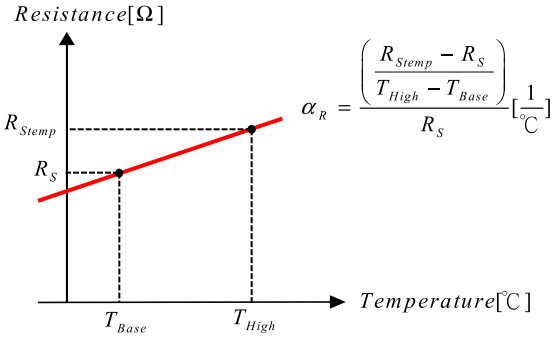

FIGURE 1. Change in resistance with temperature.

The rate of change in the resistivity according to temperature is called α_R, the resistance temperature coefficient, and a typical metal conductor has a positive temperature coefficient, as shown in Table 1. Thus, the resistance of the stator winding R_S can be expressed as a function of temperature, as shown in Equation (2). ΔT represents the difference between the current temperature and the base temperature.

$$R_S(\Delta T) = R_S\{1 + \alpha_R(T_{High} - T_{Base})\} \tag{2}$$

B. CHANGE IN THE MAGNETIC FLUX OF PERMANENT MAGNET [13], [15], [16], [18]

The residual magnetic flux density of the permanent magnet decreases with increasing temperature. The rate of change in the residual magnetic flux according to temperature the increase is called the magnetic flux temperature coefficient α_{magnet}; magnetic flux temperature coefficients of Nd-series magnets are shown in Table 2.

TABLE 2. Flux temperature coefficients of Nd-series magnets.

Material	Magnetic Temperature Coefficient [%/°C]
Alnico5	-0.02
NdFeB	-0.1
Ferrite 8	-0.2

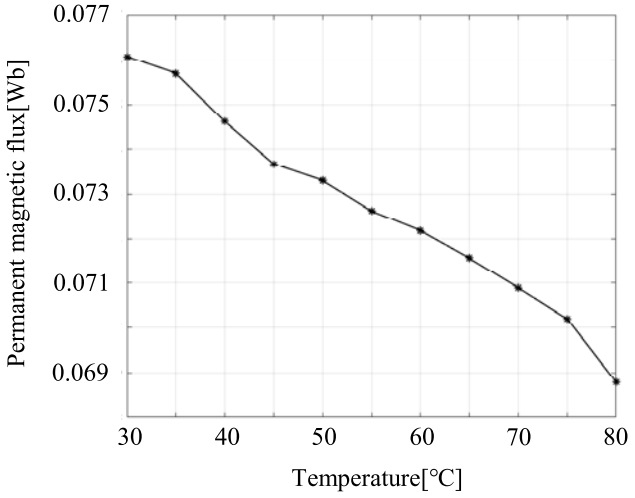

FIGURE 2. Experimental results of the magnetic flux dependence on temperature.

Therefore, according to the temperature increase, the magnetic flux density B_r and the magnetic flux ϕ_f can be expressed as functions of temperature:

$$B_r(\Delta T) = B_r(T_{Base})[1 + \alpha_{magnet}(\frac{T_{High} - T_{Base}}{100})] \quad (3)$$

$$\phi_f(\Delta T) = \oint B_r(\Delta T) \cdot ds \quad (4)$$

Fig.2 confirms the decrease in the magnetic flux due a temperature increase in an experimental motor.

After being sufficiently saturated with a chiller in the phase-open state, the target motor used in the experiment is driven at a constant speed of 1000 rpm using a load motor, representing the magnetic flux calculated through a line-to-line voltage measurement. The magnetic flux temperature coefficient A calculated through the experiment is approximately $-0.103\%/°C$, which is close to the usual value of NdFeB shown in Table 2.

C. CHANGE IN THE INDUCTANCE [3]

$$\lambda_{abc} = L_{abc}I_{abc} + \phi_{fabc}, \quad where$$
$$L_{abc} = \begin{bmatrix} L_{aa} & L_{ab} & L_{ac} \\ L_{ba} & L_{bb} & L_{bc} \\ L_{ca} & L_{cb} & L_{cc} \end{bmatrix} \quad (5)$$

The IPMSM flux linkage can be expressed as an inductance matrix as shown in Equation (5).

The IPMSM inductance matrix consists of the self-inductance and mutual inductance, as shown in Equation (6).

$$L_{aa} = L_{ls} + L_{ma} = L_{ls} + L_A - L_B \cos 2\theta_r$$
$$L_{ab} = L_{ba} = -\frac{1}{2}L_A - L_B \cos 2(\theta_r - \frac{\pi}{3}) \quad (6)$$

In addition, the inductance can be expressed as a reluctance $\Re$ and the number of turns N based on the magnetic force F [11]. Since the number of turns of the stator winding does not change, the inductance is determined by the reluctance as shown in Equation (7).

$$L = \frac{N^2}{\Re} \quad (7)$$

The magnetic path of the IPMSM consists of the core, air gap, and permanent magnet, and each transmission medium has a different permeability. The reluctance is determined by the length l, permeability μ, and cross-sectional area S as shown in Equation (8).

$$\Re = \frac{l}{\mu_{Total} \cdot S}$$
$$\mu_{Total} = \mu_{Air}(1 + \mu_{Core} + \mu_{magnet}) \quad (8)$$

Assuming that there is no change in the effective length and effective cross-sectional area of the magnetic path according to the temperature rise in Equation (8), and no change in the relative permeability of the core and air gap, the reluctance is determined by the relative permeability of the permanent magnet.

Since the relative permeability of a permanent magnet is determined by the rate of change in the relative permeability α_μ according to temperature, as shown in Equation (9), the reluctance can be expressed as a function of temperature.

$$\mu_{magnet}(\Delta T) = \mu_{magnet}(T_{Base})[1 + \alpha_\mu(T_{High} - T_{Base})] \quad (9)$$

The inductance matrix reflecting the change in reluctance due to the change in temperature is shown in Equation (10). This means that the inductance is a function of temperature.

$$L_{aa} = L_{ls} + \frac{N^2}{\Re_A(\Delta T)} - \frac{N^2}{\Re_B(\Delta T)} \cos 2\theta_r$$
$$L_{ab} = -\frac{1}{2}\frac{N^2}{\Re_A(\Delta T)} - \frac{N^2}{\Re_B(\Delta T)} \cos 2(\theta_r - \frac{\pi}{3}) \quad (10)$$

However, this inductance analysis is inappropriate for use as a general inductance equation because it is difficult to reflect the effective length and effective cross-sectional area that change depending on the shape of the rotor and stator. In addition, considering that the volume of the core increases

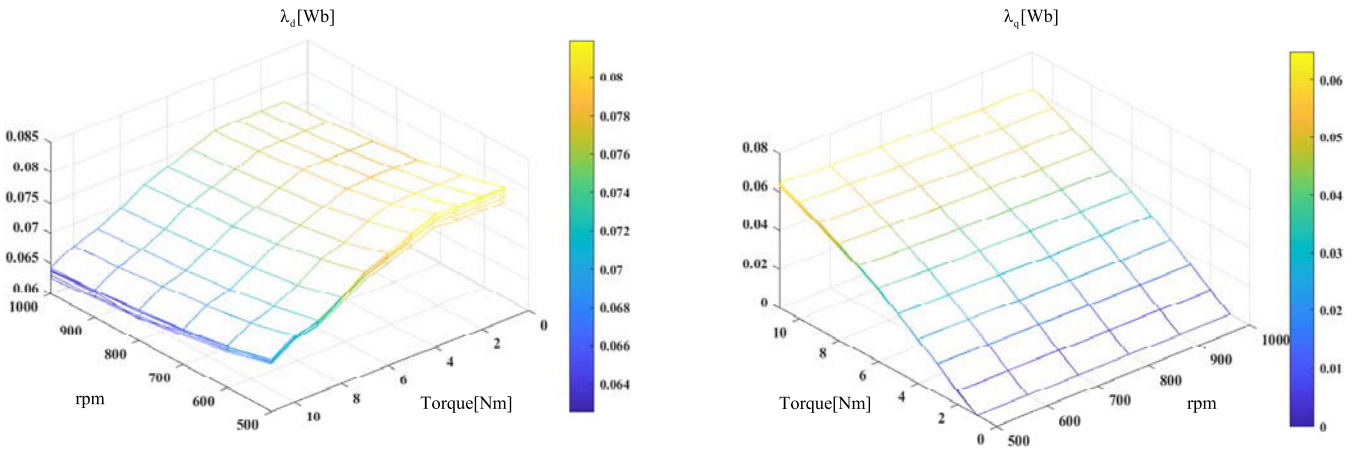

FIGURE 3. Experimental results of the flux linkage change with temperature.

according to the temperature change, and the effective length may also change accordingly, it is considered that there is a limit to calculating the change in inductance due to the temperature increase in real time and using this value for control.

D. IPMSM MODEL CONSIDERING TEMPERATURE CHANGES

The voltage equation state of a traditional IPMSM [1] is:

$$\begin{aligned} V_d &= R_S I_d - \omega_e L_q I_q = R_S I_d - \omega_e \lambda_q \\ V_q &= R_S I_q + \omega_e (L_d I_d + \phi_f) = R_S I_q + \omega_e \lambda_d \end{aligned} \tag{11}$$

The current command of the MTPA region calculated through the numerical analysis method [1] using the traditional IPMSM steady-state voltage equation is calculated as follows:

$$\begin{aligned} I_d &= \frac{\phi_f}{4(L_q - L_d)} - \sqrt{\frac{\phi_f^2}{16(L_q - L_d)^2} + \frac{I_S^2}{2}} \\ I_q &= \sqrt{I_S^2 - I_d^2} \end{aligned} \tag{12}$$

However, the above method is not an accurate current command, assuming the inductance and the magnetic flux of the permanent magnet as constants and considering the nonlinearity of the inductance and the effect of the temperature rise analyzed earlier.

Therefore, accurate estimation of the inductance of the motor and the magnetic flux of the permanent magnet is required to compensate for the torque reduced by the increase in temperature through the traditional method.

To address this problem, methods have been proposed to estimate parameters such as inductance and permanent magnet flux in real time and substitute them for the above Equation (12).

However, this method depends on the torque control performance by the performance of the observer and also has the disadvantage of requiring substantial execution time. Therefore, based on the previous analysis, we propose a new IPMSM model that can reflect temperature-driven parameter changes without the application of the observer or additional high-frequency signal injection.

Based on the parameter change analyzed in this section, it is confirmed that R_S, λ_d, and λ_q are functions of temperature. Fig.3 shows the result of confirming the change in d-q axial flux linkage according to the temperature of the experimental IPMSM.

Based on this confirmation, a new IPMSM steady-state model reflecting the temperature changes is proposed, as described in Equation (13).

R_{Stemp} is a component of the variation in the stator resistance according to the temperature, λ_{dtemp} and λ_{qtemp} are the variations in L_{dtemp} and L_{qtemp}, respectively, and the flux ϕ_{ftemp} is due to a change in temperature.

$$\begin{aligned} V_d &= (R_S + R_{Stemp}) I_d - \omega_e (L_q I_q + L_{qtemp} I_q) \\ &= (R_S + R_{Stemp}) I_d - \omega_e (\lambda_q + \lambda_{qtemp}) \\ V_q &= (R_S + R_{Stemp}) I_q \\ &\quad + \omega_e \{(L_d I_d + \phi_f) + (L_{dtemp} I_d + \phi_{ftemp})\} \\ &= (R_S + R_{Stemp}) I_q + \omega_e (\lambda_d + \lambda_{dtemp}) \end{aligned} \tag{13}$$

The proposed model is used in the process of calculating the optimal current command for torque compensation, which is the final goal of this paper, as introduced in Section III.

III. ESTIMATION OF THE FLUX LINKAGE THROUGH ACTIVE AND REACTIVE POWER

Since the iron loss is modeled [10] as a higher-order polynomial, real-time estimation is difficult.

In addition, since iron loss modeling depends on operating conditions and test environments, it is practically impossible to estimate the copper loss and iron loss and use those values for compensation. Therefore, in this paper, we focus on compensating for the error between the effective power calculated through the LUT developed at the base temperature and the

effective power calculated in real time by considering the total loss.

A. DEFINITION OF THE LOSS RESISTANCE THROUGH ACTIVE POWER

The active and reactive power of the IPMSM can be defined through the IPMSM phasor diagram shown in Fig.4. The active power is used to calculate a loss resistance introduced later, and the reactive power is used to verify the validity after estimating the flux linkage through the calculated loss resistance.

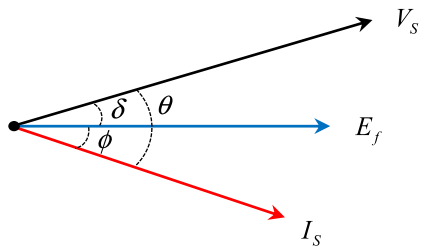

FIGURE 4. Phasor diagram.

The active power P_{Total} of the IPMSM is represented by Equation (14).

$$\begin{aligned} P_{Total} &= V_S I_S \cos(\phi + \delta) \\ &= V_S I_S(\cos\phi\cos\delta - \sin\phi\sin\delta) \\ &= V_S(I_q\cos\delta + I_d\sin\delta) = \frac{3}{2}(V_q I_q + V_d I_d) \end{aligned} \quad (14)$$

Then, Equation (15) can be obtained by substituting Equation (11), the steady-state equation of the traditional IPMSM, into Equation (14).

$$\begin{aligned} P_{Total} &= \frac{3}{2}(V_q I_q + V_d I_d) \\ &= \frac{3}{2}\{R_S(I_d^2 + I_q^2) + \omega_e(\lambda_d I_q - \lambda_q I_d)\} \end{aligned} \quad (15)$$

Substituting Equation (13) of the IPMSM, reflecting the temperature change proposed in Section II, into Equation (14) results in the following expression:

$$\begin{aligned} P_{Total} &= \frac{3}{2}(V_q I_q + V_d I_d) \\ &= \frac{3}{2}\{R_S(I_d^2+I_q^2)+\omega_e(\lambda_d I_q - \lambda_q I_d)+R_{Stemp}(I_d^2 + I_q^2) \\ &\quad + \omega_e(\lambda_{dtemp} I_q - \lambda_{qtemp} I_d)\} \end{aligned} \quad (16)$$

This shows that the decrease in the output power torque is caused by the fluctuating components λ_{dtemp} and λ_{qtemp} of the flux linkage in accordance with the temperature change, and in this paper, this decrease is regarded as a loss due to the temperature change. In the absence of a change in the motor temperature, the output torque T_e is the same as the torque command T_e^* based on the LUT at the base temperature, so the mechanical output can be expressed as follows:

$$P_{mechanical} = \frac{3}{2}\omega_e(\lambda_d I_q - \lambda_q I_d) = \omega_m T_e^* \quad (17)$$

Thus, the loss can be expressed as follows by separating the mechanical output from the total active power.

$$P_{Loss} = P_{Total} - P_{mechanical} \quad (18)$$

Even if a parameter changes according to an increase in temperature, the size of a current command by the LUT does not change, so a loss may be equivalent to a voltage drop by resistance R_{Loss}, and this paper defines this resistance as a loss resistance.

The equation representing the loss as the loss resistance and current is as follows:

$$\begin{aligned} &P_{Loss} \\ &= \frac{3}{2}(R_S(I_d^2+I_q^2)+R_{Stemp}(I_d^2+I_q^2)+\omega_e(\lambda_{dtemp}I_q-\lambda_{qtemp}I_d)) \\ &= \frac{3}{2}(R_S(I_d^2+I_q^2)+R_{Stemp}(I_d^2+I_q^2)+(V_{\lambda temp}I_q + V_{\lambda temp}I_d)) \\ &= \frac{3}{2}(R_S(I_d^2+I_q^2)+R_{Stemp}(I_d^2+I_q^2) + (R_{\lambda temp}I_q^2 + R_{\lambda temp}I_d^2)) \\ &= \frac{3}{2}(R_S(I_d^2+I_q^2) + R_{Stemp}(I_d^2+I_q^2) + R_{\lambda temp}(I_d^2+I_q^2)) \\ &= R_{Loss}I_S^2 \text{ (where, } R_{Loss} = R_S + R_{Stemp} + R_{\lambda temp}) \end{aligned} \quad (19)$$

In the above equation, R_{Stemp} represents the stator resistance fluctuation according to the temperature rise, and $R_{\lambda temp}$ represents the loss equivalent resistance due to the fluctuation of the flux linkage due to that temperature rise. The loss resistance can be calculated in real time by excluding the mechanical output from the active power, as shown below:

$$R_{Loss} = \frac{P_{Total} - P_{mechanical}}{I_S^2} = \frac{\frac{3}{2}(V_q I_q + V_d I_d) - \omega_m T_e^*}{I_S^2} \quad (20)$$

B. ESTIMATION OF THE FLUX LINKAGE BASED ON THE LOSS RESISTANCE

Fig.5 shows the voltage drop due to the loss resistance of IPMSM at steady state using a vector diagram. Based on

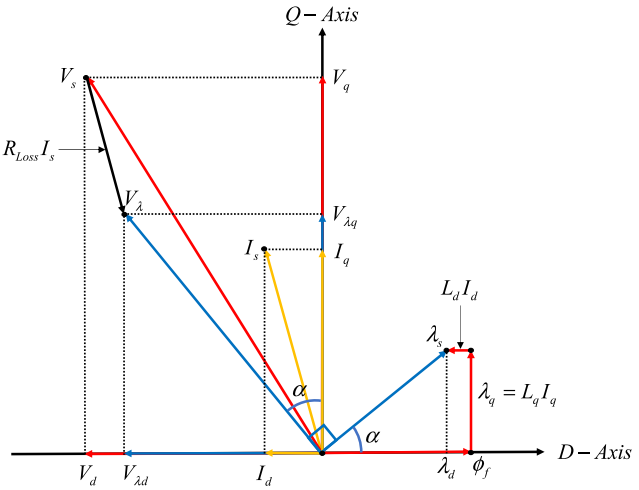

FIGURE 5. Vector diagram of the IPMSM steady state [19].

this diagram, only the voltages $V_{\lambda d}$ and $V_{\lambda q}$ contribute to the generation of the flux linkage, excluding the voltage drop caused by the loss resistance. Accordingly, the voltage generating the flux linkage can be expressed as:

$$V_\lambda = \sqrt{(V_{\lambda d}^2 + V_{\lambda q}^2)} \tag{21}$$

where $V_{\lambda d}$ and $V_{\lambda q}$ are:

$$\begin{aligned} V_{\lambda d} &= V_d - R_{Loss} I_d \\ V_{\lambda q} &= V_q - R_{Loss} I_q \end{aligned} \tag{22}$$

Based on Equations (20)-(22), λ_d and λ_q can be estimated using the magnitude of the flux linkage λ_S and angle α. Since only the voltage excluding the voltage drop due to loss from the total voltage contributes to the generation of the flux linkage, λ_S and the angle α are expressed as:

$$\lambda_S = \frac{\sqrt{(V_{\lambda d}^2 + V_{\lambda q}^2)}}{\omega_e}, \quad \alpha = \arctan(\frac{V_{\lambda d}}{V_{\lambda q}}) \tag{23}$$

Therefore, the estimated d-q axis flux linkages λ_{dEst} and λ_{qEst} are:

$$\begin{aligned} \lambda_{dEst} &= \lambda_d + \lambda_{dtemp} = \lambda_s \cos\alpha \\ \lambda_{qEst} &= \lambda_q + \lambda_{qtemp} = \lambda_s \sin\alpha \end{aligned} \tag{24}$$

C. VERIFICATION OF THE FLUX LINKAGE ESTIMATION THROUGH THE REACTIVE POWER

The flux linkage estimated through the active power may be verified through the reactive power. From Fig.4, the reactive power Q_{Total} of the IPMSM is represented by Equations (25).

$$\begin{aligned} Q_{Total} &= V_S I_S \sin(\phi + \delta) \\ &= V_S I_S (\sin\phi\cos\delta + \cos\phi\sin\delta) \\ &= V_S (I_d \cos\delta + I_q \sin\delta) = \frac{3}{2}(V_q I_d - V_d I_q) \end{aligned} \tag{25}$$

Substituting Equation (13) related to the proposed voltage into Equation (25) yields:

$$\begin{aligned} Q_{Total} &= \frac{3}{2}(V_q I_d - V_d I_q) \\ &= \frac{3}{2}\{(R_S + R_{Stemp}) I_q I_d + \omega_e(\lambda_d + \lambda_{dtemp}) I_d \\ &\quad - (R_S + R_{Stemp}) I_d I_q + \omega_e(\lambda_q + \lambda_{qtemp}) I_q\} \\ &= \frac{3}{2}\omega_e\{(\lambda_d + \lambda_{dtemp}) I_d + (\lambda_q + \lambda_{qtemp}) I_q\} \end{aligned} \tag{26}$$

Through Equation (26), it can be confirmed that the loss due to stator resistance is not reflected in the reactive power and consists of the flux linkages. The reactive power calculated using the voltage is Q_{Cal}, the reactive power calculated using the estimated flux linkage is Q_{Est}, and the error Q_{Err} can be defined as the difference between Q_{Cal} and Q_{Est}:

$$\begin{aligned} Q_{Cal} &= \frac{3}{2}(V_q I_d - V_d I_q) \\ Q_{Est} &= \frac{3}{2}\omega_e(\lambda_{dEst} I_d + \lambda_{qEst} I_q) \end{aligned} \tag{27}$$

If Q_{Err} calculated with Equation (27) is small, the estimated result can be determined to be reasonable.

IV. CALCULATION OF THE COMPENSATION CURRENT THROUGH THE LAGRANGE MULTIPLIER METHOD

The impact of a temperature change on the torque curve and MTPA is presented in Fig.6 based on the analysis in Section II. *Te(High)* and *Te(Low)* represent the same torque line [12], [17].

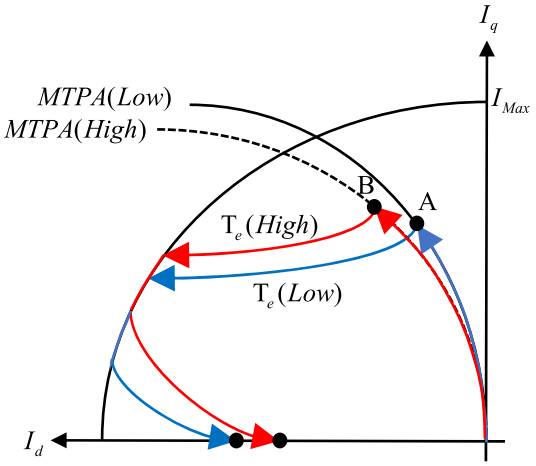

FIGURE 6. Operating point change as influenced by temperature.

In this section, a method for moving to the optimal operating point is proposed using the flux linkage and the estimated torque calculated through the loss resistance proposed in the previous section. The proposed method consists of the following steps: Firstly, Lagrange multiplier method is applied to the mathematical model of IPMSM to derive an equation for the optimal operating point. This equation is comprised of the flux linkage and the estimated torque. Then, the calculated flux linkage and estimated torque obtained through the loss resistance are substituted into the derived equation. Subsequently, the movement from the current operating point

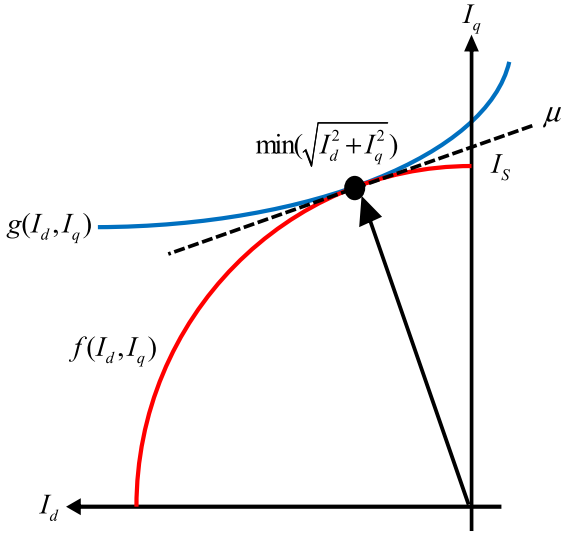

FIGURE 7. Application of Lagrange method in the d-q coordinate system.

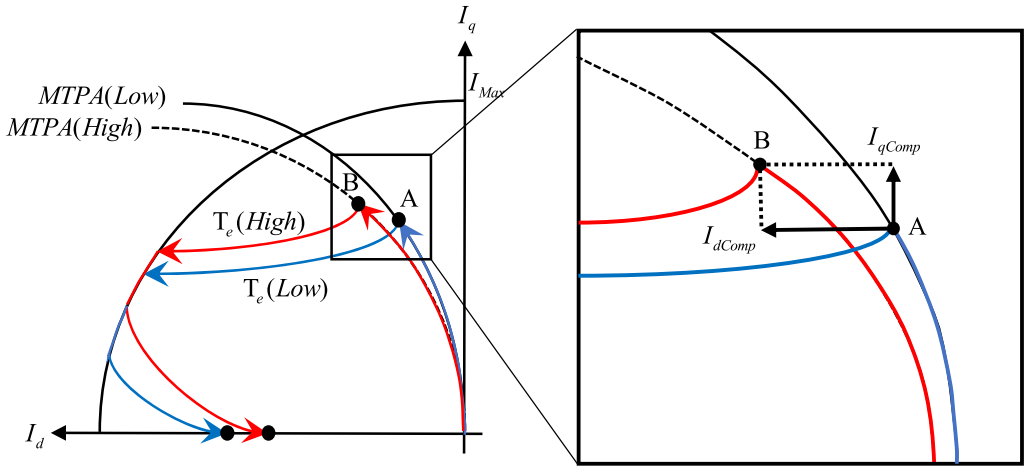

FIGURE 8. The d-q axis current for torque error compensation.

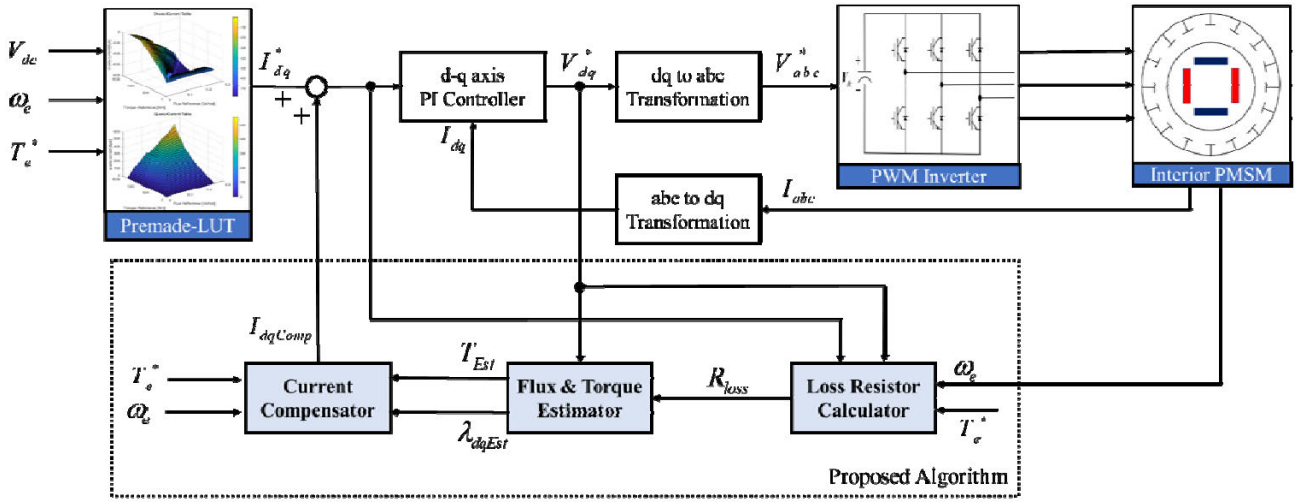

FIGURE 9. Block diagram of the proposed algorithm.

to the optimal operating point becomes possible by adding the calculated compensation current to the current command through this process.

The Lagrange multiplier method is used to find the maximum or minimum value of a function by considering both objective functions and constraints. The intuitive understanding for the Lagrange multiplier method has been depicted in Fig.7 in the d-q coordinate system of IPMSM. The minimum value is located at the circumference of a circle with radius I_S, and the slopes of functions $f(I_d, I_q)$ and $g(I_d, I_q)$ are equal. Hence, the optimal operating point of the IPMSM can be determined using the Lagrange multiplier method as described below.

The objective function $f(I_d, I_q)$ and constraint $g(I_d, I_q)$ can be expressed by the following equations:

$$f(I_d, I_q) = (I_d^2 + I_q^2) \tag{28}$$

$$g(I_d, I_q) = T_e - \frac{3}{2}\frac{P}{2}(\lambda_d I_q - \lambda_q I_d) \tag{29}$$

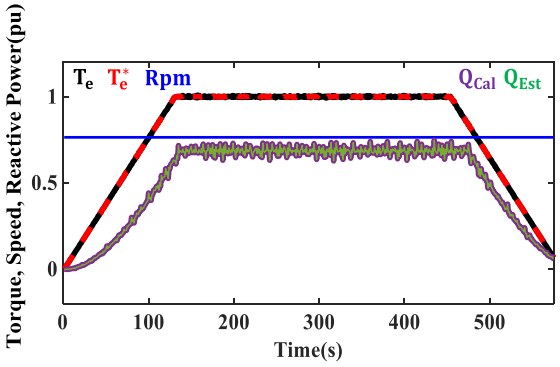

FIGURE 10. Simulation results of the calculated and estimated reactive power.

The same slope is expressed as:

$$\nabla f(I_d, I_q) = \mu \nabla g(I_d, I_q) \tag{30}$$

In Equation (30), μ means that the slope vectors of two functions $f(I_d, I_q)$ and $g(I_d, I_q)$ are related to each other by a

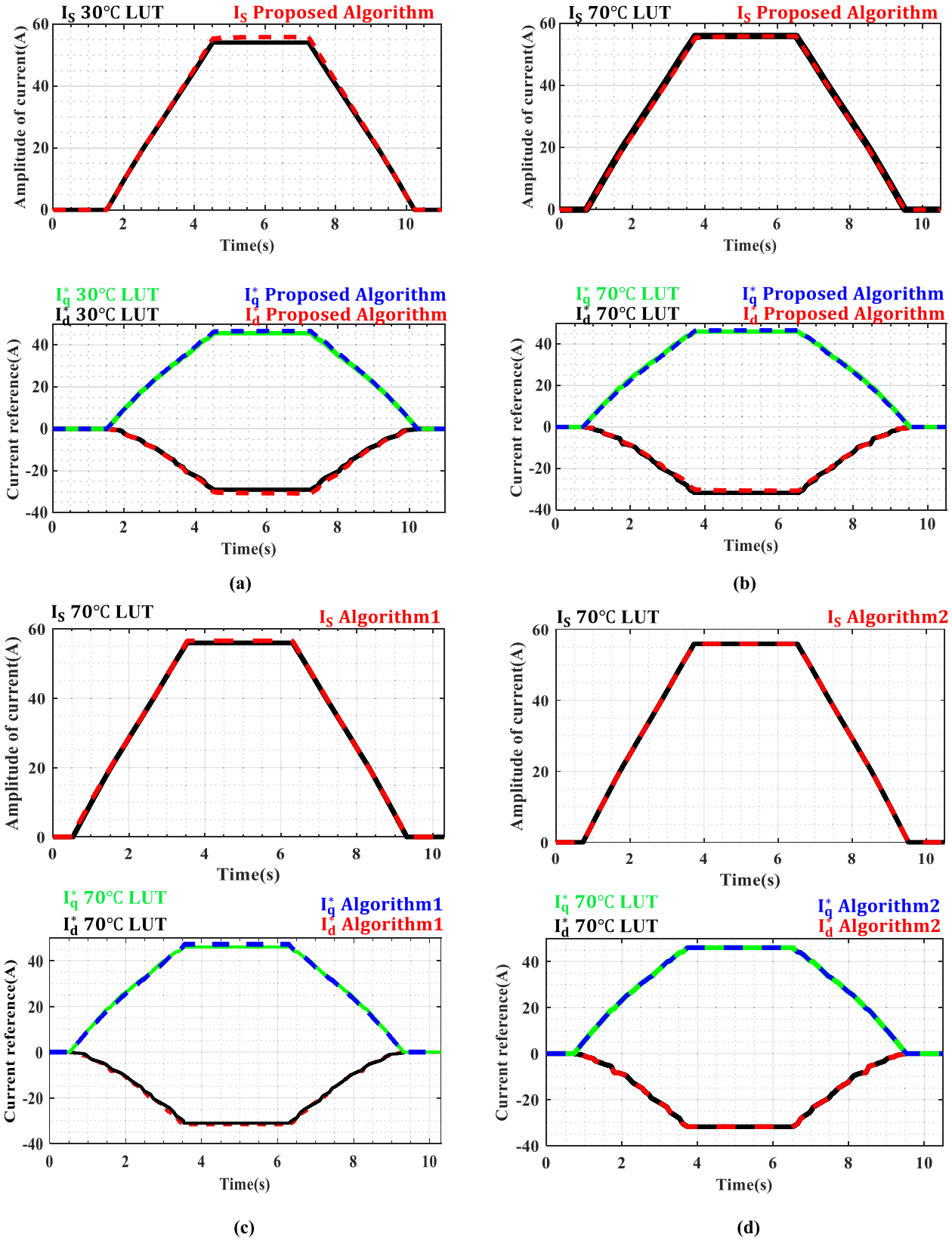

FIGURE 11. Comparison of the LUT and proposed algorithm based on the simulation results under 70°C temperature condition: (a) 30°C LUT versus the proposed algorithm, (b) 70°C LUT versus proposed algorithm, (c) 70°C LUT versus algorithm 1, (d) 70°C LUT versus algorithm 2.

multiplicative constant, where the coordinates of points with the same slope can be calculated by defining a new function, such as Equation (31), based on the two functions.

$$h(I_d, I_q, \mu) = f - \mu g \tag{31}$$

$$\nabla h = \left(\frac{\partial h}{\partial I_d}, \frac{\partial h}{\partial I_q}, \frac{\partial h}{\partial \mu}\right) = 0 \tag{32}$$

Equation (32) shows that the minimum value exists at a point where the value of the partial derivative is zero, as the factors I_d, I_q, and μ of the function are independent of each other. Solving Equation (32) yields:

$$\frac{\partial h}{\partial I_d} = 2I_d - \frac{3}{2}\frac{N_P}{2}\mu\lambda_q = 0 \tag{33}$$

$$\frac{\partial h}{\partial I_q} = 2I_q - \frac{3}{2}\frac{N_P}{2}\mu\lambda_d = 0 \tag{34}$$

$$\frac{\partial h}{\partial \mu} = T_e - \frac{3}{2}\frac{N_P}{2}(\lambda_d I_q - \lambda_q I_d) = 0 \tag{35}$$

The above equation for μ is summarized as follows:

$$\mu = \frac{2I_d}{\frac{3}{2}\frac{N_P}{2}\lambda_q}, \quad \mu = \frac{-2I_q}{\frac{3}{2}\frac{N_P}{2}\lambda_d} \tag{36}$$

In Equation (36) are combined to eliminate the Lagrange constant μ, as follows:

$$I_q = \frac{\lambda_q T_e}{\lambda_d^2 + \lambda_q^2} \tag{37}$$

$$I_d = -I_q \frac{\lambda_q}{\lambda_d} \tag{38}$$

If the magnetic fluxes estimated through the loss resistance proposed in Section III are λ_{dEst} and λ_{qEst}, the error between the estimated torque and the torque command can be expressed as:

$$T_{eEst} = \frac{3}{2}\frac{N_P}{2}(\lambda_{dEst} I_q - \lambda_{qEst} I_d) \tag{39}$$

$$T_{eErr} = T_e^* - \frac{3}{2}\frac{N_P}{2}(\lambda_{dEst} I_q - \lambda_{qEst} I_d) \tag{40}$$

If the Equations(37) and (38) is replaced with a torque command, an estimation torque, and an estimation flux linkage, as shown in Fig.8, the operating point A on the LUT can be used as an origin, and the d-q-axis currents I_{dComp} and I_{qComp} that compensate for T_{Err} can be obtained as:

$$I_{qComp} = \frac{\lambda_{qEst}(T_e^* - T_{Est})}{\lambda_{dEst}^2 + \lambda_{qEst}^2} \tag{41}$$

$$I_{dComp} = -I_{qComp}\frac{\lambda_{qEst}}{\lambda_{dEst}} \tag{42}$$

By adding the compensation current size calculated through Equations (41) and (42) in the current command of the LUT at base temperature, the operating point A at base temperature can be moved to the modified operating point B due to the temperature rise, with A as the origin.

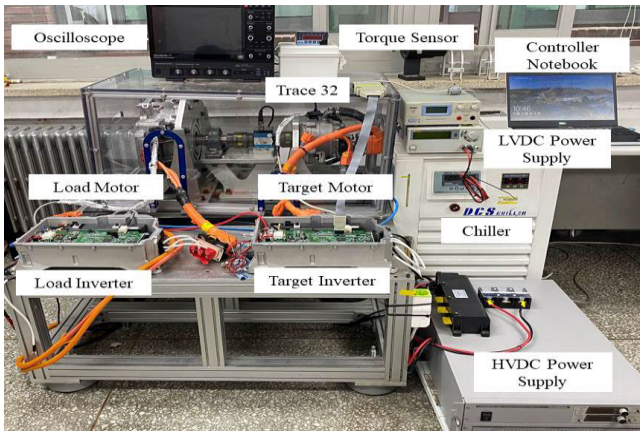

FIGURE 12. Experiment environment.

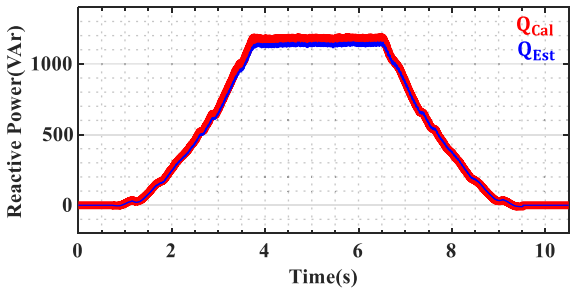

FIGURE 13. Experimental results for the calculation and reactive power estimation.

V. SIMULATION AND EXPERIMENTAL RESULTS

A. SIMULATION RESULT

In this paper, MATLAB/Simulink is used to verify the proposed algorithm, and the rate of change in the magnetic flux and phase resistance according to temperature are reflected.

The IPMSM model parameters used in the simulation are shown in Table 3; the magnetic flux temperature coefficient α_{magnet} is $-0.1\%/°C$, and the resistance temperature coefficient α_R is 0.004 Ω/°C.

TABLE 3. Nominal IPMSM parameters.

Parameter	Value
Number of pole pairs	6
Maximum power	7.3 kW
Maximum torque	21.4 Nm
Rated speed	3260 rpm
DC-link voltage	240 V

The block diagram of the proposed algorithm is shown in Fig.9 and consists of a prewritten LUT at the base temperature, loss resistance calculators, magnetic flux and torque estimators, and a current command compensator.

To verify the validity of the proposed algorithm, the prewritten LUT at 30°C, LUT interpolation at each temperature [8], algorithm 1 [5], algorithm 2 [9], and the current

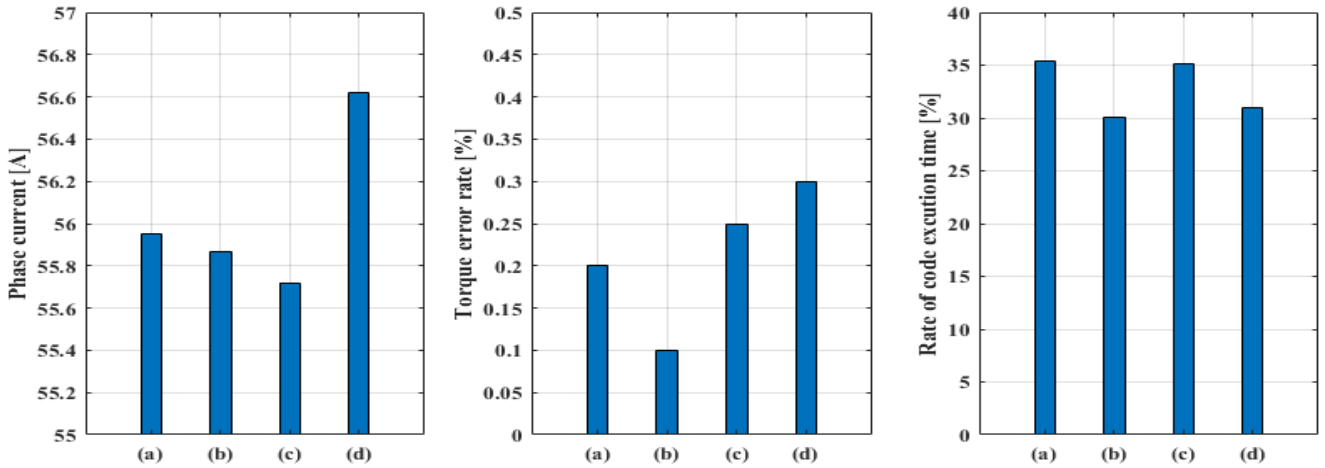

FIGURE 14. Performance comparison by each algorithm: (a) LUT interpolation at each temperature, (b) proposed algorithm, (c) algorithm 1, (d) algorithm 2.

command to which the proposed algorithm is applied are compared.

Fig.10 shows the error of the calculated reactive power described in Section III and the estimated reactive power from the proposed algorithm.

Table 4 shows the error rate, where the maximum error is 0.77%, the minimum error is 0.002%, and the average error is 0.38%, so the result of the magnetic flux estimation upon applying the proposed method can be considered reasonable.

TABLE 4. Error rate of the reactive power estimation.

Reactive Power Error	Value [%]
Maximum	0.77
Average	0.384
Minimum	0.002

Fig.11 shows a comparison between each algorithm and the results of the proposed algorithm under the 70°C -temperature condition.

To compensate for the torque error caused by the increase in the motor temperature, the magnitude of the compensated d-q current command increases in the proposed algorithm relative to the d-q axis current command of the 30°C LUT.

It is confirmed that each algorithm has a current error of less than 1% compared to the 70°C LUT.

B. EXPERIMENTAL RESULT

Fig.12 shows the experimental configuration environment. The parameters of the experimental IPMSM are the same as those in Table 3.

An indirect method is adopted to use a chiller to saturate the motor temperature, and an experiment is conducted enough time after the chiller was operated.

Fig.13 compares the reactive power proposed in Section III to the experimental results to verify the validity of the flux linkage estimation through loss resistance. The maximum error rate is 4.17%, the average error rate is 3.49%, and the minimum error rate is 2.86%, so the result of the estimation is reasonable.

TABLE 5. Error rate of the reactive power estimation.

Unit: Var	Q_{Cal}	Q_{Est}	Q_{Error}	Error rate
Maximum	1190.3	1156.2	34.1	4.17%
Average	1176.6	1135.5	41.1	3.49%
Minimum	1162.2	1113.7	48.5	2.86%

TABLE 6. Comparison of the LUT and proposed algorithm based on the experimental results under 70°C temperature condition.

	I_d [A]	I_q [A]	I_S [A]	Torque[Nm]
30°C LUT	-29.02	45.65	54.08	19.38
(a)	-31.79	46.04	55.95	20.04
(b)	-30.75	46.65	55.87	19.98
(c)	-31.11	46.23	55.72	19.94
(d)	-30.19	47.91	56.62	20.05

Table 6 shows the experimental results. When using only single LUT at 30°C, it is confirmed that the output torque decreases as previously analyzed, and when each algorithm is applied, the reduced output torque is compensated. The phase difference of the current is small when each algorithm is used, but all torque error rates are within 1%, 3.1% in a single LUT at 30°C, 0.2% in the LUT interpolation at each temperature, 0.1% in the proposed algorithm, 0.25% in algorithm 1, and 0.3% in algorithm 2. This is shown in Fig.17. And Fig.14 represents the size of the current, torque precision, and code execution time rate of each algorithm. The proposed algorithm consumes less current by up to 0.75A

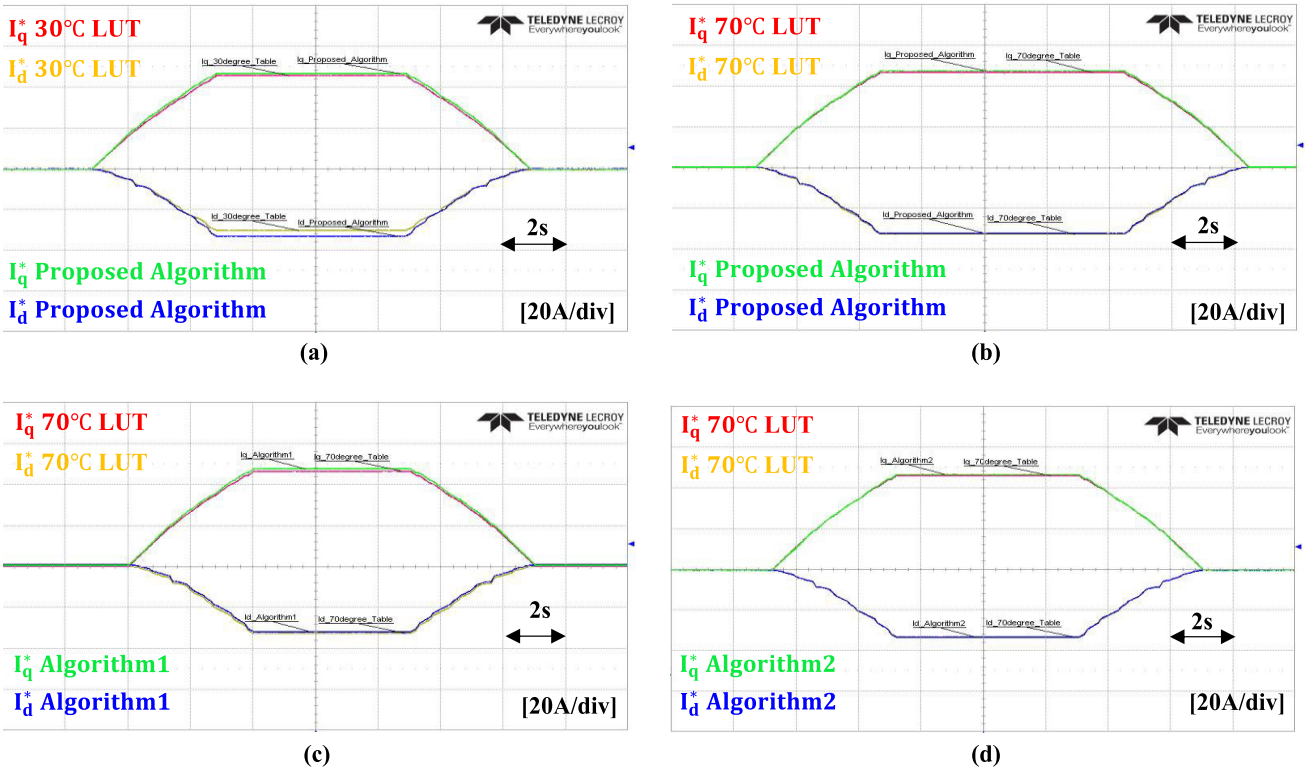

FIGURE 15. Comparison of the LUT and proposed algorithm based on the experimental results under 70°C temperature condition: (a) 30°C LUT versus proposed algorithm, (b) 70°C LUT versus proposed algorithm, (c) 70°C LUT versus algorithm 1, (d) 70°C LUT versus algorithm 2.

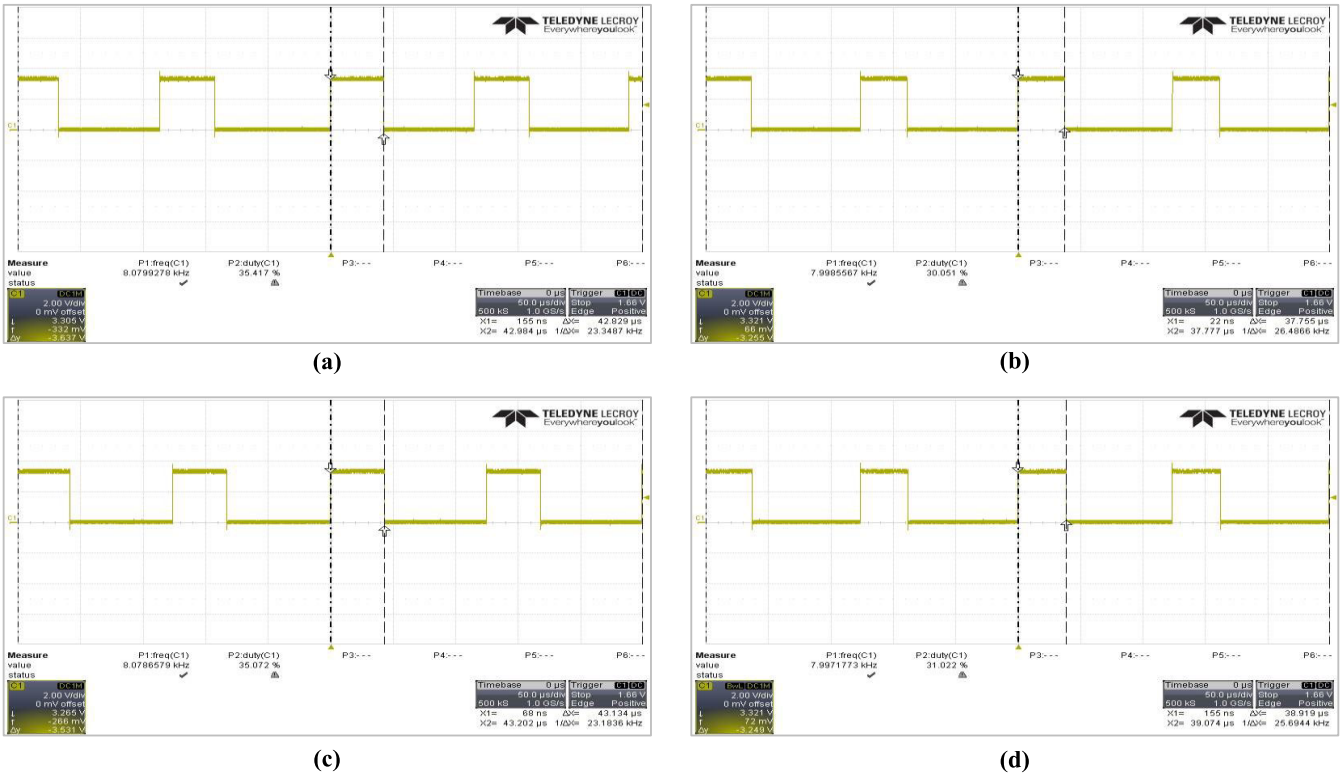

FIGURE 16. Code execution time of each algorithm: (a) LUT interpolation at each temperature, (b) proposed algorithm, (c) algorithm 1, (d) algorithm 2.

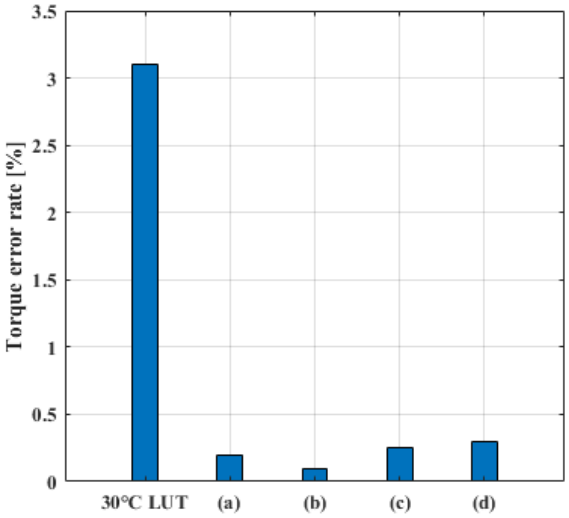

FIGURE 17. Comparison of the torque error rate of each algorithm: (a) LUT interpolation at each temperature, (b) proposed algorithm, (c) algorithm 1, (d) algorithm 2.

compared to other algorithms, improves the torque precision by up to 0.2%, and decreases the code execution time by up to 5%.

Fig.15(a) shows a comparison between the 30°C LUT and the proposed algorithm under the 70°C -temperature condition. Like the simulation result, the magnitude of the d-q-axis current command that is compensated through the proposed algorithm increases relative to the 30°C LUT to compensate for a torque error caused by the motor temperature increase.

Fig.15(b), (c) and (d) show a comparison between the 70°C LUT and the each algorithm under the 70°C temperature condition. When the proposed algorithm is applied, there is a small difference in the d-q-axis current command phase relative to the 70°C LUT, but it is negligible, and no error arises in the magnitude of the current command or torque.

Fig.16 shows the code execution time rate of each algorithm.

VI. CONCLUSION

In this paper, the active power loss is calculated using a single LUT at the base temperature and the loss resistance is defined.

Then, the d-q axis flux linkage and torque are estimated based on the loss resistance. Moreover, a torque error-compensation method based on the temperature change is proposed using the Lagrange multiplier method, which is a mathematical optimization method.

The proposed algorithm does not require additional parameters observer and high frequency injection for torque compensation, which eliminates the reduction in control performance due to the parameter observer and the decrease in available voltage caused by the high frequency injection.

The proposed algorithm is validated through simulation and experiment; the optimal operating point can be selected using only a single LUT at the base temperature. It is also confirmed that the proposed algorithm has a higher torque precision and lower execution time than other algorithms. This is expected to result in a reduction in the cost of physical and time-related costs for writing LUTs for each temperature and the possibility of adding additional algorithms due to the reduction in execution time.

NOMENCLATURE

Symbols

R	Stator resistance.
L	Stator inductance.
$\Re$	Reluctance.
F	Electromagnetic force.
I	Stator current.
H	Magnetic field strength.
B_r	Residual magnetic flux density.
N_P	Number of turns.
P	Active power.
Q	Reactive power.
λ	Flux linkage.
ϕ_f	Magnetic flux.
ω_e	Electrical rotor speed.
T_e	Electromagnetic torque.
∇	Gradient operator.
Δ	Differential value.
∂	Partial differential operator.

Subscripts

a, b, c	The a-, b-, and c-axes in the three-phase reference frame.
d, q	Direct and quadrature axes in the rotor reference frame.
S	Synthetic value.
Est	Estimated value.
Cal	Calculated value.
$Comp$	Compensated value.
Err	Error value.
$temp$	Value of change with temperature.
λ	Value by flux linkage.

Superscript

$*$	Reference value.

REFERENCES

[1] J.-M. Kim and S.-K. Sul, "Speed control of interior permanent magnet synchronous motor drive for the flux weakening operation," *IEEE Trans. Ind. Appl.*, vol. 33, no. 1, pp. 43–48, Jan. 1997, doi: 10.1109/28.567075.

[2] T. Sebastian, "Temperature effects on torque production and efficiency of PM motors using NdFeB magnets," *IEEE Trans. Ind. Appl.*, vol. 31, no. 2, pp. 353–357, Mar./Apr. 1995, doi: 10.1109/28.370284.

[3] H.-S. Jung, H. Kim, S.-K. Sul, and D. J. Berry, "Temperature estimation of IPMSM by using fundamental reactive energy considering variation of inductances," *IEEE Trans. Power Electron.*, vol. 36, no. 5, pp. 5771–5783, May 2021, doi: 10.1109/TPEL.2020.3028084.

[4] S. Li, D. Han, and B. Sarlioglu, "Modeling of interior permanent magnet machine considering saturation, cross coupling, spatial harmonics, and temperature effects," *IEEE Trans. Transport. Electrific.*, vol. 3, no. 3, pp. 682–693, Sep. 2017, doi: 10.1109/TTE.2017.2679212.

[5] S.-Y. Cho, W.-G. Shin, J.-S. Park, and W.-H. Kim, "A torque compensation control scheme of PMSM considering wide variation of permanent magnet temperature," *IEEE Trans. Magn.*, vol. 55, no. 2, pp. 1–5, Feb. 2019, doi: 10.1109/TMAG.2018.2864649.
[6] H.-S. Kim and S.-K. Sul, "Real-time torque control of IPMSM under flux variations," *IEEE J. Emerg. Sel. Topics Power Electron.*, vol. 10, no. 3, pp. 3345–3356, Jun. 2022, doi: 10.1109/JESTPE.2020.3032463.
[7] S.-Y. Jung, J. Hong, and K. Nam, "Current minimizing torque control of the IPMSM using Ferrari's method," *IEEE Trans. Power Electron.*, vol. 28, no. 12, pp. 5603–5617, Dec. 2013, doi: 10.1109/TPEL.2013.2245920.
[8] Y.-S. Kim and S.-K. Sul, "Torque control strategy of an IPMSM considering the flux variation of the permanent magnet," in *Proc. IEEE Ind. Appl. Annu. Meeting*, Sep. 2007, pp. 1301–1307, doi: 10.1109/07IAS.2007.202.
[9] D. Kang, J. Hwang, G. Lee, H. Lim, and W. Jin, "Improvement of torque accuracy of interior permanent magnet synchronous motor considering temperature variation," *J. Magn.*, vol. 26, no. 3, pp. 311–321, Sep. 2021.
[10] I. Jeong, B.-G. Gu, J. Kim, K. Nam, and Y. Kim, "Inductance estimation of electrically excited synchronous motor via polynomial approximations by least square method," *IEEE Trans. Ind. Appl.*, vol. 51, no. 2, pp. 1526–1537, Mar./Apr. 2015, doi: 10.1109/TIA.2014.2339634.
[11] W.-H. Kim, M.-J. Kim, K.-D. Lee, J.-J. Lee, J.-H. Han, T.-C. Jeong, S.-Y. Cho, and J. Lee, "Inductance calculation in IPMSM considering magnetic saturation," *IEEE Trans. Magn.*, vol. 50, no. 1, pp. 1–4, Jan. 2014, doi: 10.1109/TMAG.2013.2277586.
[12] C. Choi, W. Lee, S. O. Kwon, and J. P. Hong, "Experimental estimation of inductance for interior permanent magnet synchronous machine considering temperature distribution," *IEEE Trans. Magn.*, vol. 49, no. 6, pp. 2990–2996, Jun. 2013, doi: 10.1109/TMAG.2013.2238550.
[13] S. Li, D. Han, and B. Sarlioglu, "Impact of temperature variation on fuel economy of electric vehicles and energy saving by using compensation control," in *Proc. IEEE Transp. Electrific. Conf. Expo. (ITEC)*, Jun. 2018, pp. 702–707, doi: 10.1109/ITEC.2018.8450144.
[14] S. Li, B. Sarlioglu, S. Jurkovic, N. R. Patel, and P. Savagian, "Analysis of temperature effects on performance of interior permanent magnet machines for high variable temperature applications," *IEEE Trans. Ind. Appl.*, vol. 53, no. 5, pp. 4923–4933, Oct. 2017, doi: 10.1109/TIA.2017.2700473.
[15] S. Li, B. Sarlioglu, S. Jurkovic, N. R. Patel, and P. Savagian, "Comparative analysis of torque compensation control algorithms of interior permanent magnet machines for automotive applications considering the effects of temperature variation," *IEEE Trans. Transport. Electrific.*, vol. 3, no. 3, pp. 668–681, Sep. 2017, doi: 10.1109/TTE.2017.2684080.
[16] A. Rabiei, T. Thiringer, M. Alatalo, and E. A. Grunditz, "Improved maximum-torque-per-ampere algorithm accounting for core saturation, cross-coupling effect, and temperature for a PMSM intended for vehicular applications," *IEEE Trans. Transport. Electrific.*, vol. 2, no. 2, pp. 150–159, Jun. 2016, doi: 10.1109/TTE.2016.2528505.
[17] F. Marignetti and V. D. Colli, "Thermal analysis of an axial flux permanent-magnet synchronous machine," *IEEE Trans. Magn.*, vol. 45, no. 7, pp. 2970–2975, Jul. 2009, doi: 10.1109/TMAG.2009.2016415.
[18] J. Fan, "Thermal analysis of permanent magnet motor for the electric vehicle application considering driving duty cycle," *IEEE Trans. Magn.*, vol. 46, no. 6, pp. 2493–2496, Jun. 2010, doi: 10.1109/TMAG.2010.2042043.
[19] G.-H. Lee, S.-I. Kim, J.-P. Hong, and J.-H. Bahn, "Torque ripple reduction of interior permanent magnet synchronous motor using harmonic injected current," *IEEE Trans. Magn.*, vol. 44, no. 6, pp. 1582–1585, Jun. 2008, doi: 10.1109/TMAG.2008.915776.

HYUN-JUN BAEK received the B.S. degree in electronics engineering from Kookmin University, Seoul, South Korea, in 2016, where he is currently pursuing the Ph.D. degree in automotive engineering. His research interests include the inverter design and permanent magnet AC motor control.

SOON-HO KWON received the B.S. degree in electrical engineering from Myongji University, Gyeonggi-do, South Korea, in 2017, and the M.S. and Ph.D. degrees in automotive engineering from Kookmin University, in 2019 and 2022, respectively. Currently, he is with Hyundai Mobis, where he develops inverter system for automotive. His research interests include power converter/inverter design and permanent magnet AC motor control.

DEUK-WON YOON received the B.S. and M.S. degrees in automotive engineering from Kookmin University, Seoul, South Korea, in 2021 and 2023, respectively. Currently, he is with Hyundai Mobis, where he develops inverter system for automotive. His research interests include the power converter/inverter design and permanent magnet AC motor control.

DO-HYUN KANG (Graduate Student Member, IEEE) received the B.S. degree in electrical and computer engineering from Sungkyunkwan University, Suwon, South Korea, in 2013. He is currently pursuing the Ph.D. degree in electrical and computer engineering. From 2013 to 2017, he was an Electrical Engineer with the Rotating Machinery Division, Hyundai Electrics (Formerly Hyundai Heavy Industries), South Korea. His research interests include multi-physical design and system-level optimization of electric machines.

GEUN-HO LEE received the B.S. and M.S. degrees in electrical engineering and the Ph.D. degree in automotive engineering from Hanyang University, Seoul, South Korea, in 1992, 1994, and 2010, respectively. From 1994 to 2002, he was with the LG Industrial Research Institute, where he developed inverter system for elevators. Since 2011, he has been a Professor in automotive engineering with Kookmin University. His current research interests include the advanced control of electric machines and electric vehicles.

HEE-SUN LIM received the bachelor's degree in mechanical and automotive engineering and the Ph.D. degree in automotive engineering from Kookmin University, Seoul, South Korea, in 2015 and 2022, respectively. She is currently a Postdoctoral Fellow with the Graduate School of Automotive Engineering, Kookmin University. Her research interests include advanced control of electromechanical and automotive inverters.